

Supporting Information

Electronic Structure Regulation on the Ultra-thin MOF-derived NiSe₂/NiS₂@NC Heterojunction for Promoting the Hydrogen Evolution Reaction

Kebin Lu^[a,†], Jianpeng Sun^[a,†], Huakai Xu^[a], Chuanhai Jiang^[a], Weifeng Jiang^[a], Fangna Dai*^[a], Hong Wang*^[b], Hongguo Hao*^[c]

^aCollege of Science, School of Materials Science and Engineering China University of Petroleum (East China) Qingdao, Shandong, 266580, P. R. China. E-mail: fndai@upc.edu.cn.

^bCollege of Materials Science and Engineering, Beijing University of Chemical Technology, Beijing, P. R. China. Beijing University of Chemical Technology Beijing, P. R. China. E-mail: wanghong@mail.buct.edu.cn.

^cShandong Provincial Key Laboratory of Chemical Energy Storage and Novel Cell Technology, School of Chemistry and Chemical Engineering, Liaocheng University, Liaocheng 252059, China. E-mail: hhg207@126.com

[†]These authors contributed equally.

Table of contents

S1 Electrochemical measurements	1
Preparation of working electrodes	2
Electrochemical measurements	2
S2 Density functional theory (DFT) calculations	2
S3 Material characterization	3
S4 The catalytic performance of the material	8
S5 Density functional theory (DFT) calculations model	10
S6 Comparison of electrocatalytic performance of materials	12
References.....	13

S1 Electrochemical measurements

Preparation of working electrodes

The working electrode was prepared in the following way: 5.0 mg of sample was dissolved in the mixture of Nafion solution (50 μL , 5 wt%) and ethanol (950 μL). The mixture was sonicated for 30 min to form a homogeneous ink. Subsequently, 5 μL of solution was dripped on the glassy carbon electrode at room temperature. The loading amount of the catalyst was 0.17 $\text{mg}\cdot\text{cm}^{-2}$. Before taking measurements, the GCE loaded with active materials was allowed to dry at room temperature for one hour.

Electrochemical measurements

All HER tests in this article were performed with a typical three-electrode system (Gamry INTERFACE 1000 T) at room temperature. The synthetic samples, a graphite rod and a calomel electrode (SCE) were separately used as the working electrode, the counter electrode and the reference electrode. The test solution was 0.5 M H_2SO_4 and 1.0 M KOH solution. All test results were corrected by the formula ($\text{ERHE} = \text{ESCE} + 0.0592\text{pH} + 0.242 \text{ V}$) and corrected for the iR -drop. Before the HER test, the working electrode was scanned with cyclic voltammetry (CV) until the sample is stable. Linear sweep voltammetry (LSV) were recorded at 5 $\text{mV}\cdot\text{s}^{-1}$. Electrochemical impedance spectroscopy (EIS) measurements were performed in the frequency range of 10^{-5} Hz to 10^{-2} Hz with amplitude of 5 mV. To obtain the C_{dl} value, CV curves were collected at 0.35 to 0.45 V (vs. RHE) with the scan rates of 20 to 100 $\text{mV}\cdot\text{s}^{-1}$, respectively. The electrochemical double layer capacitance (C_{dl}) values by using the linear slopes of curves of $\Delta J/2$ vs. scan rate for calculation. The ECSA and the normalized current density were calculated using the double layer capacitance (C_{dl}), according to the equation $\text{ECSA} = C_{\text{dl}}/C_s$, $j_{\text{normalized}} = j/\text{ECSA}$, where C_s is the specific capacitance of the material, j is current density. Tafel plots are calculated to understand the reaction mechanism of HER performance according to the Tafel equation $\eta = b \lg j + a$ (j stands for current density and b for slope). The stability was evaluated by using CV at 100 $\text{mV}\cdot\text{s}^{-1}$ for 2000 cycles. The long-term stability test was completed using chronopotentiometric measurement without iR drop compensation.

S2 Density functional theory (DFT) calculations

Density functional theory (DFT) calculations were performed using Vienna ab initio Simulation Package (VASP) with the generalized gradient approximation (GGA) parameterized by Perdew, Burke and Ernzerhof (PBE) for the exchange correlation functional^[1-3]. An energy cutoff of 300 eV is used for all calculations. We use a 2×2×1 k-point mesh for NiS₂ and NiSe₂, and a 2×1×1 k-point mesh for NiS₂/NiSe₂.

The 128-atom-sized supercell of Ni₂₄S₄₀/Ni₂₄Se₄₀ interface model was chosen with 5-layer cross-section thick of NiS₂ and NiSe₂ part respectively. Supercells are composed of 8-atomiclayer-thick slabs separated by ~15 Å of vacuum perpendicular to the surface to prevent spurious interactions due to periodic boundary conditions, and we only allow the top two layers to be relaxed. Structures are relaxed until forces on each atom are less than 10⁻⁴ eV/Å.

The adsorption energy of H atom on the catalyst surface was calculated, which is expressed as:

$$\Delta G_{H^*} = \Delta E_H + \Delta E_{ZPE} - T\Delta S$$

Where ΔE_H , ΔE_{ZPE} , and ΔS are the adsorption energy of hydrogen atom, zero-point energy change and entropy difference of H* for the two states. We have chosen 0.24 eV as the value of ($\Delta E_{ZPE} - T\Delta S$), and $\Delta G_{H^*} = \Delta E_H + 0.24$ eV.

S3 Material characterization

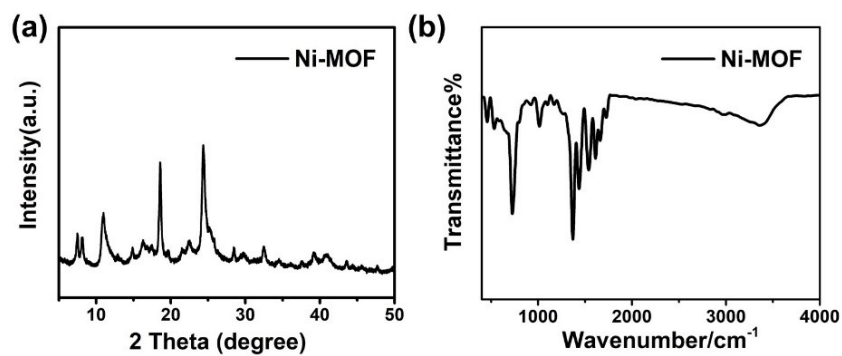


Figure S1 (a) XRD pattern and (b) FT-IR spectra of ultrathin layered MOF.

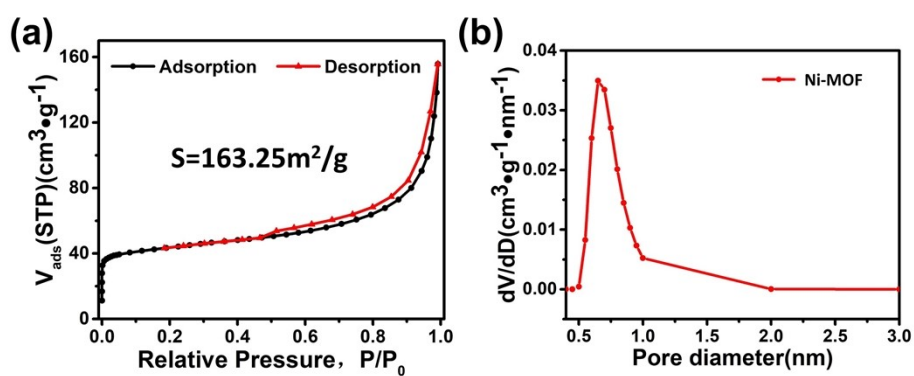


Figure S2. (a) N₂ adsorption-desorption isotherms and (b) pore size distribution curve of ultrathin layered MOF.

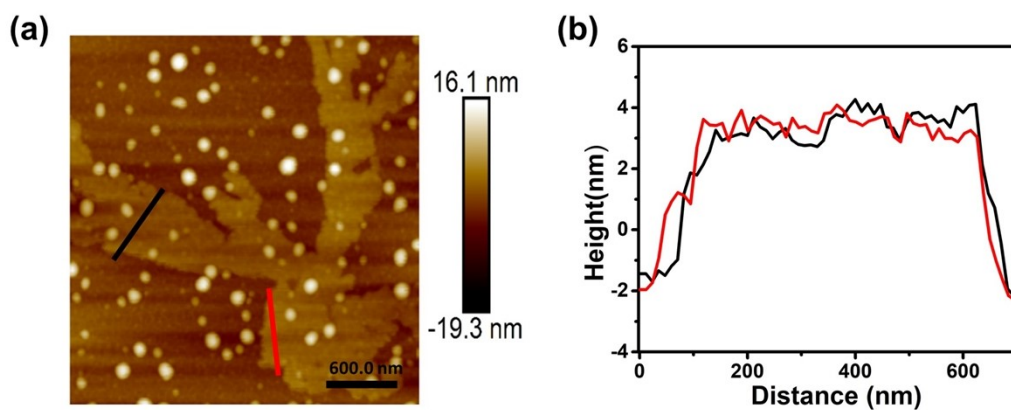


Figure S3. AFM images of ultrathin MOF nanosheets

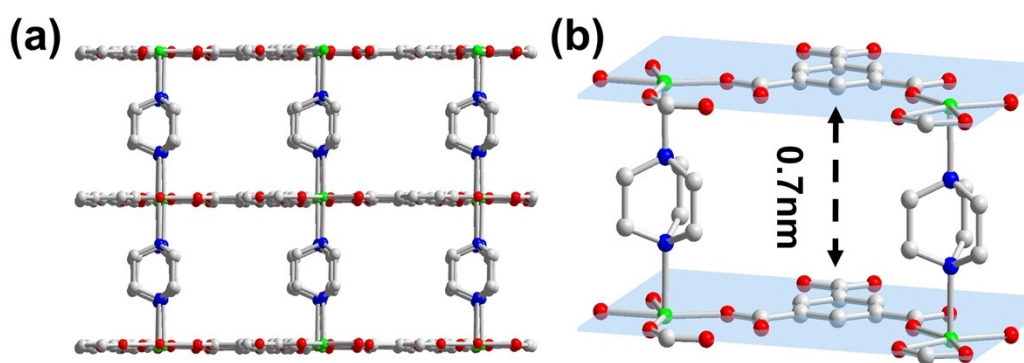


Figure S4 The pillar-layered structure of ultrathin layered MOF.

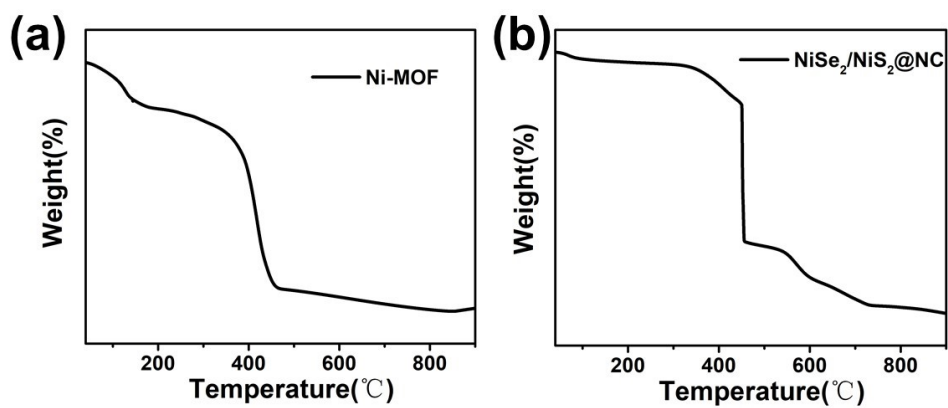


Figure S5 (a) TGA curve of Ni-MOF performed in the N₂ atmosphere. (b) TGA curve of NiSe₂/NiS₂@NC nanomaterials performed in the O₂ atmosphere.

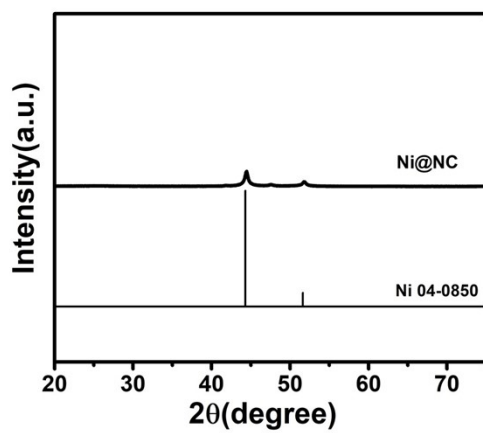


Figure S6 XRD pattern of Ni@NC

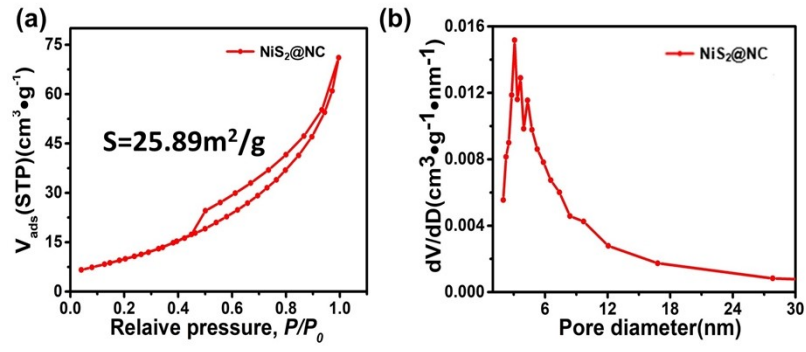


Figure S7 (a) N_2 adsorption–desorption isotherms and (b) pore size distribution curve of $NiS_2@NC$.

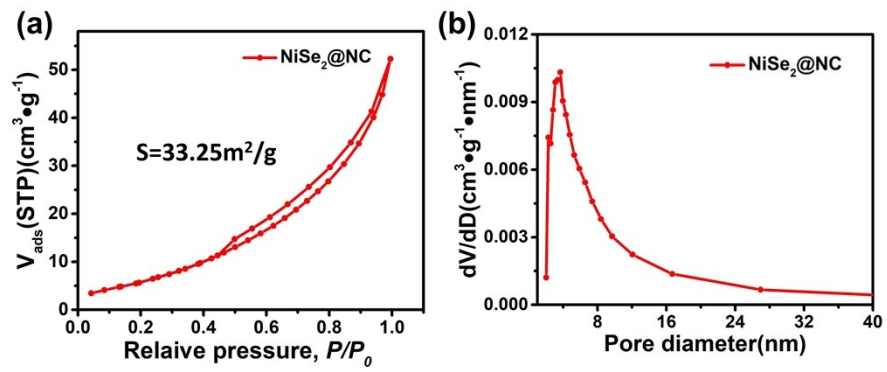


Figure S8 (a) N_2 adsorption–desorption isotherms and (b) pore size distribution curve of $NiSe_2@NC$.

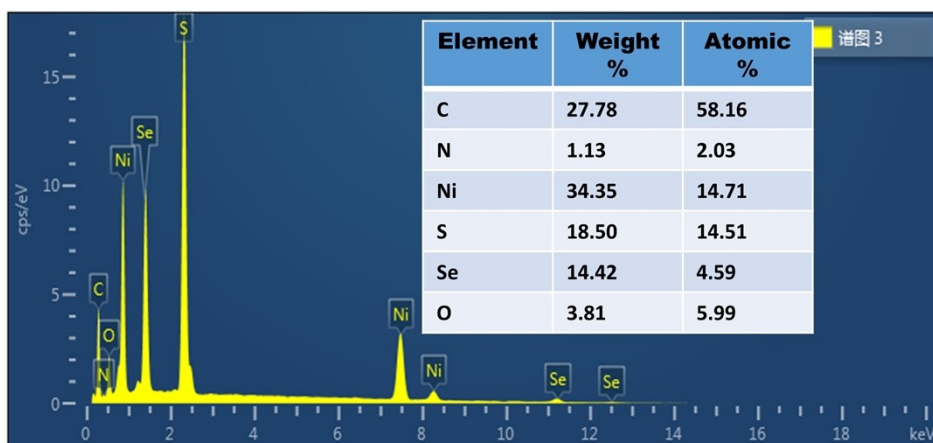


Figure S9. Energy dispersive spectra of NiSe₂/NiS₂@NC nanomaterials.

S4 The catalytic performance of the material

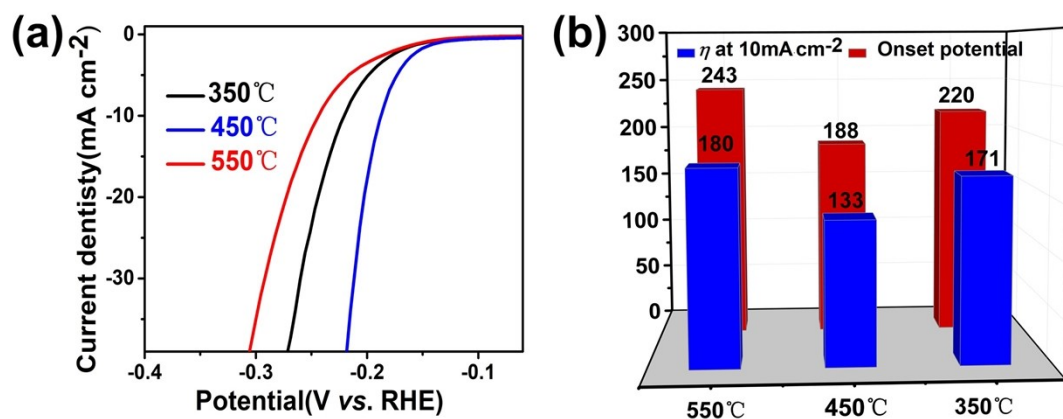


Figure S10 Electrochemical performance in 0.5 M H₂SO₄ solution. (a) LSV curves of 350°C, 450°C and 550°C. (b) The onset potential and overpotential (η) of the as-prepared electrodes at the current density of 10 mA·cm⁻².

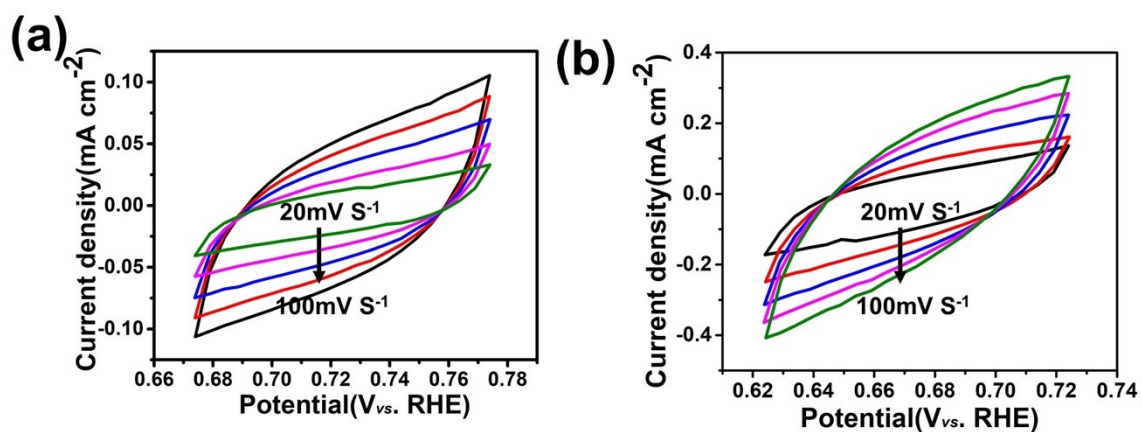


Figure S11. Electrochemical performance in 0.5 M H₂SO₄ solution. (a) The CV curves of NiS₂@NC. (b) The CV curves of NiSe₂@NC.

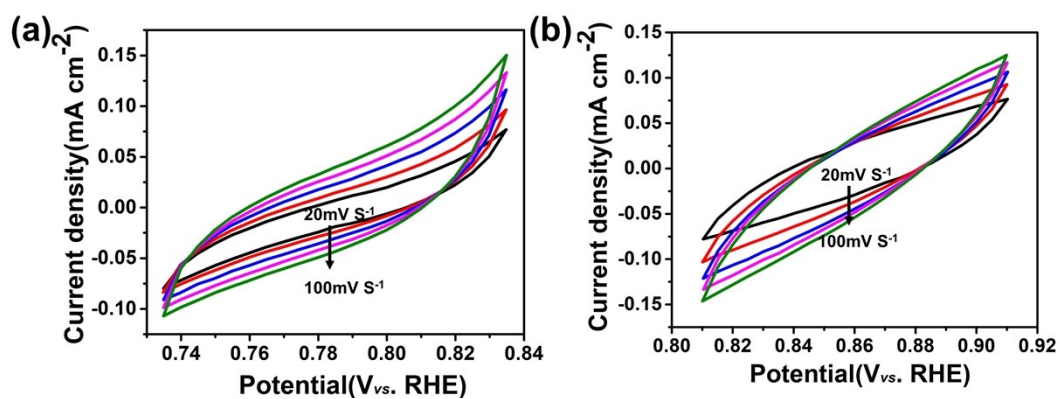


Figure S12 Electrochemical performance in 1.0 M KOH solution. (a) The CV curves of NiS₂@NC. (b) The CV curves of NiSe₂@NC.

S5 Density functional theory (DFT) calculations model

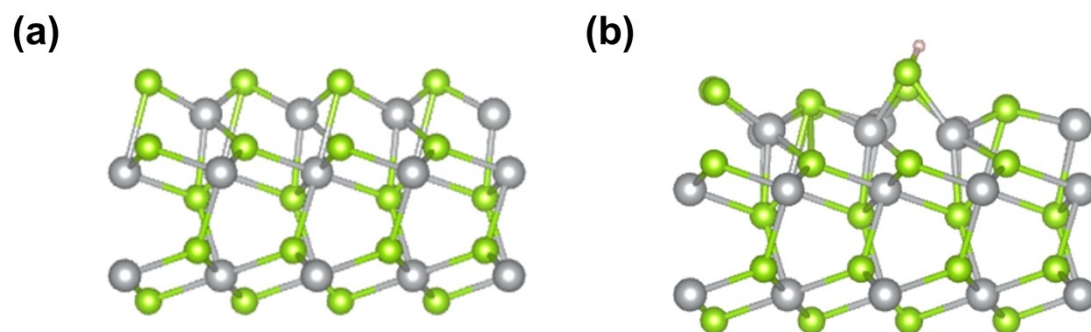


Figure S13 The theoretical models of (a) NiSe₂ and (b) schematic models of NiSe₂ with H⁺ adsorbed on its surface

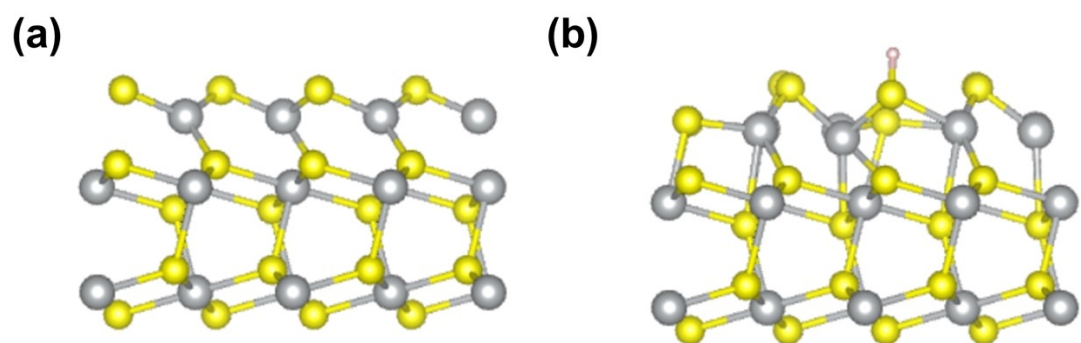


Figure S14 The theoretical models of (a) NiS₂ and (b) schematic models of NiS₂ with H⁺ adsorbed on its surface

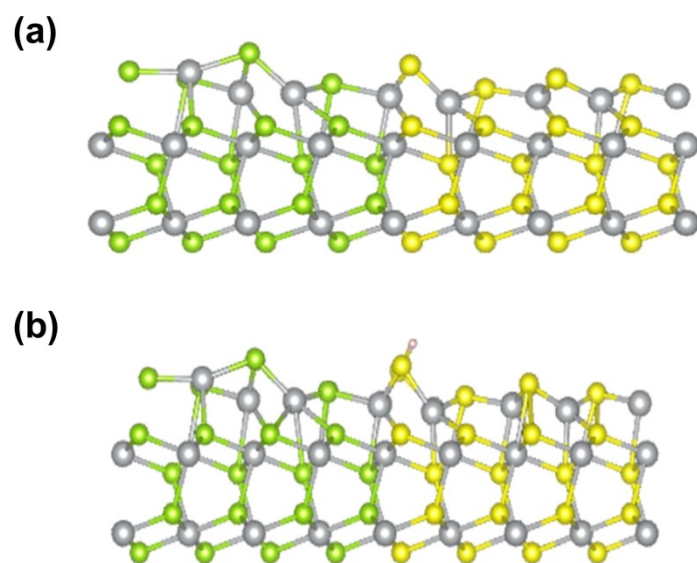


Figure S15 The theoretical models of (a) NiSe₂/NiS₂ and (b) schematic models of NiSe₂/NiS₂ with H⁺ adsorbed on its surface

	ΔE	ΔG
NiS ₂	-303.206	-1.114
NiS ₂ -H	-307.796	
NiSe ₂	-277.729	-0.519
NiSe ₂ -H	-281.723	
NiSe ₂ /NiS ₂	-576.629	-0.352
NiSe ₂ /NiS ₂ -H	-580.456	

Figure S16 The free energy change of the HER process on NiS₂, NiSe₂, NiSe₂/NiS₂.

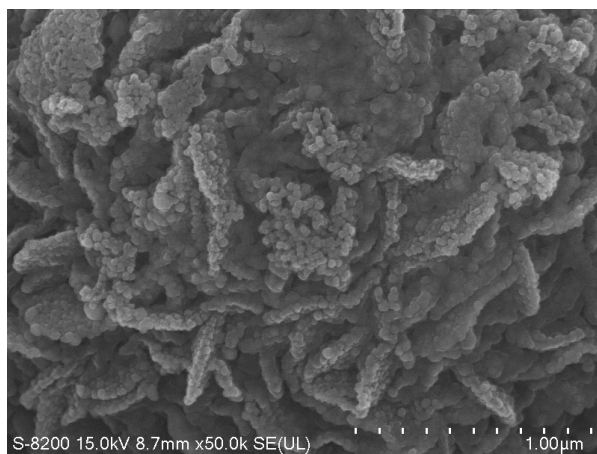


Figure S17. Scanning electron microscope image of NiSe₂/NiS₂@NC

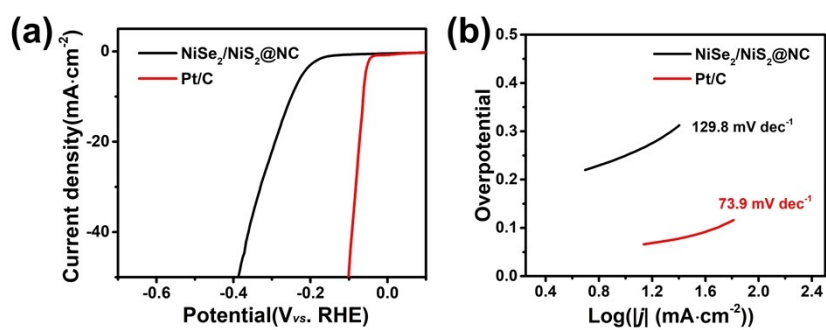


Figure S18. The LSV polarization curves and corresponding Tafel plots of NiSe₂/NiS₂@NC and Pt/C in 1.0 M PBS solution.

S6 Comparison of electrocatalytic performance of materials

Table S1. Comparison of HER catalytic activity of different catalysts in 0.5 M H₂SO₄

HER catalysts	E ₁₀ (mV)	Tafel slope (mV·dec ⁻¹)	Electrolyte	Ref.
NiSe ₂ /NiS ₂ @NC	188	46	0.5 M H ₂ SO ₄	This work
NiS ₂ /MoS ₂ HNW	235	58	0.5 M H ₂ SO ₄	[4]
MoS ₂ /MoO ₂	210	129	0.5 M H ₂ SO ₄	[5]
NiS ₂ -MoS ₂	210	56	0.5 M H ₂ SO ₄	[6]
MoS ₂ /MoO ₂	240	76	0.5 M H ₂ SO ₄	[7]
Ni@NC/MoS ₂ -P	315	118.2	0.5 M H ₂ SO ₄	[8]
CoS _{1.097} /MoS ₂	249	75	0.5 M H ₂ SO ₄	[9]
NiSe ₂ @NG-140	201	36.1	0.5 M H ₂ SO ₄	[10]
Ni _{0.85} Se/GS	200	81	0.5 M H ₂ SO ₄	[11]
NiSe ₂ /C	205	38.7	0.5 M H ₂ SO ₄	[12]
MoS ₂	210	97	0.5 M H ₂ SO ₄	[13]

Table S2 Comparison of HER catalytic activity of different catalysts in 1 M KOH

HER catalysts	E ₁₀ (mV)	Tafel slope (mV·dec ⁻¹)	Electrolyte	Ref.
NiSe ₂ /NiS ₂ @NC	211	93.2	1.0 M KOH	This work
0.2CoSe ₂ /MoSe ₂	218	76	1.0 M KOH	[14]
CoS _{1.097} /MoS ₂	249	75	1.0 M KOH	[9]
WS ₂ -graphene	255	100	1.0 M KOH	[15]
2H-MoS ₂ /CC	226	62	1.0 M KOH	[16]
MoS ₂ /C HCSs	476	274	1.0 M KOH	[17]
Co _{0.85} Se@NC	230	125	1.0 M KOH	[18]
Co@NCNTs-800	240	83	1.0 M KOH	[19]

Co ₃ O ₄ -CuO	288	65	1.0 M KOH	[20]
NiS ₂ HMSs	232	102	1.0 M KOH	[21]

References

- [1] G. Kresse and J. Furthmuller, *Phys. Rev. B.*, 1996, **54**, 11169-11186.
- [2] G. Kresse and J. Furthmuller, *Comp. Mater. Sci.*, 1996, **6**, 15-50.
- [3] J. Perdew, K. Burke and M. Ernzerhof, *Phys. Rev. Lett.*, 1996, **77**, 3865-3868.
- [4] P. Y. Kuang, T. Tong, K. Fan and J. Yu, *ACS Catal.*, 2017, **7**, 6179-6187.
- [5] C. -L. Wu, P. -C. Huang, S. Brahma, J. -L. Huang and S. -C. Wang, *Ceram. Int.*, 2017, **43**, S621-S627.
- [6] X. Zhou, Y. Liu, H. Ju, B. Pan, J. Zhu, T. Ding, C. Wang and Q. Yang, *Chem Mater.*, 2016, **28**, 1838-1846.
- [7] L. Yang, W. Zhou, D. Hou, K. Zhou, G. Li, Z. Tang, L. Lia, and S. Chen, *Nanoscale*, 2015, **7**, 5203.
- [8] S. Hao, L. Chen and C. Yu, *ACS Energy Lett.*, 2019, **4**, 952-959.
- [9] J. Sun, Z. Huang, T. Huang, X. Wang, P. Wang, Y. Zong, F. Dai and D. Sun, *ACS Appl. Energy Mater.*, 2019, **2**, 7504-7511.
- [10] W. Li, B. Yu, Y. Hu, X. Wang, D. Yang and Y. Chen, *ACS Sustainable Chem Eng.*, 2019, **7**, 4351-4359.
- [11] X. Wu, D. He, H. Zhang, H. Li, Z. Li, B. Yang, Z. Lin, L. Lei and X. Zhang, *Int. J. Hydrog. Energy.*, 2016, **41**, 10688-94.
- [12] D. Song, H. Wang, X. Wang, B. Yu and Y. Chen, *Electrochim. Acta.*, 2017, **254**, 230-237.
- [13] W. Zhang, Z. Xie, X. Wu, M. Sun, X. Deng, C. Liu, Z. Liu and Q. Huang, *Mater. Lett.*, 2018, **230**, 232-235.
- [14] G. Zhao, P. Li, K. Rui, Y. Chen, S. Dou and W. Sun, *Chem. Eur. J.*, 2018, **24**, 11158-11165.
- [15] J. Yang, D. Voiry, S. Ahn, J. Kang, A. Y. Kim, M. Chhowalla and H. S. Shin, *Angew. Chem. Int. Ed. Engl.*, 2013, **52**, 13751.
- [16] Z. Liu, L. Zhao, Y. Liu, Z. Gao, S. Yuan, X. Li, N. Li and S. Miao, *Appl. Catal. B*, 2019, **246**, 296-302.
- [17] Y. Yang, M. Luo, Y. Xing, S. Wang, W. Zhang, F. Lv, Y. Li, Y. Zhang, W. Wang and S. Guo, *Adv. Mater.*, 2018, **30**, 1706085.

- [18] T. Meng, J. Qin, S. Wang, D. Zhao, B. Mao and M. Cao, *J. Mater. Chem. A*, 2017, **5**, 7001.
- [19] J. -S. Li, B. Du, Z. -H. Lu, Q. -T. Meng and J. -Q. Sha, *New J. Chem.*, 2017, **41**, 10966.
- [20] A. Tahira, Z. H. Ibupoto, M. Willander and O. Nur, *Int. J. Hydrog. Energy.*, 2019, **44**, 26148-26157.
- [21] T. Tian, L. Huang, L. Ai and J. Jiang, *J. Mater. Chem. A*, 2017, **5**, 20985.